



Final Year Project Report

Construction and Testing of a 3D printed Ellipsometer on a Budget

Name: Ishka Ó Cathluain

Student No.: 19449436

Class: PHA4

Date: 11th April 2023

Supervisor: Dr. Paul Swift

Declaration

Name: Ishka Ó Cathluain
Student ID Number: 19449436
Programme: Physics with Astronomy
Module Code: PS451
Assignment Title: Final Year Project
Submission Date: 11th April 2023

I understand that the University regards breaches of academic integrity and plagiarism as grave and serious.

I have read and understood the DCU Academic Integrity and Plagiarism Policy. I accept the penalties that may be imposed should I engage in practice or practices that breach this policy.

I have identified and included the source of all facts, ideas, opinions, viewpoints of others in the assignment references. Direct quotations, paraphrasing, discussion of ideas from books, journal articles, internet sources, module text, or any other source whatsoever are acknowledged and the sources cited are identified in the assignment references.

I declare that this material, which I now submit for assessment, is entirely my own work and has not been taken from the work of others save and to the extent that such work has been cited and acknowledged within the text of my work.

I have used the DCU library referencing guidelines (available at: <http://www.library.dcu.ie/LibraryGuides/Citing&ReferencingGuide/player.html>) and/or the appropriate referencing system recommended in the assignment guidelines and/or programme documentation.

By signing this form or by submitting this material online I confirm that this assignment, or any part of it, has not been previously submitted by me or any other person for assessment on this or any other course of study.

By signing this form or by submitting material for assessment online I confirm that I have read and understood DCU Academic Integrity and Plagiarism Policy (available at: <http://www.dcu.ie/registry/examinations/index.shtml>).

Name: Ishka Ó Cathluain
Date: 9 April 2023

Abstract

3D printing technology has advanced considerably in the past decade and is now at a stage where it can be used to print complex precision instruments to aid in research. In this project, an ellipsometer was printed and used to measure the complex refractive index and film thickness for a thin gold film as well as several other samples, using both fixed and variable angle of incidence techniques. These samples were then measured with a commercial ellipsometer, and the results were compared. The thin gold films thickness as measured with the printed ellipsometer was measured to be $27.3 \pm 4\text{nm}$ and its complex refractive index $\tilde{N} = 0.42 \pm 0.08 + 3.6 \pm 0.2i$. The commercial ellipsometer measured the thickness to be $29.2 \pm 0.3\text{nm}$ and the known refractive index of gold is $\tilde{N} = 0.15557 + 3.6024i[1]$.

Acknowledgments

Firstly, I would like to thank my project supervisor Dr. Paul Swift, and Dr. Tony Cafolla for being there to answer my questions and give guidance when needed. I want to also thank Patrick Wogan for his enthusiasm in helping me with the printing and just in general for helping me find all those odds and ends that were needed. Finally, I want to thank my mother for giving me the encouragement to keep at this.

List of Figures

2.1	Light incident on a thin film of thickness d.[2]	3
2.2	Theoretical plot of Ellipsometry Angles vs AoI for a thick gold film at a wavelength of 650nm and $\tilde{N}_{Au} = 0.1556 + 3.6i$.	4
2.3	Theoretical plot of Ellipsometry Angles vs AoI for a thin gold film(10nm) at a wavelength of 650nm and $\tilde{N}_{Au} = 0.1556 + 3.6i$.	5
2.4	Basic diagram of the components of an ellipsometer[3].	5
3.1	CAD model of the two goinometer arms attached to the main body of the ellipsometer[4].	9
3.2	CAD model of the ellipsometer sample mount[4].	9
3.3	CAD model of the ellipsometer polariser mount with the worm drive.	10
3.4	Laser calibration measurements of Intensity as a function of polariser angle.	13
3.5	Plot of $Cos^2(\theta)$ vs Normalised Intensity with line of best fit.	13
4.1	Fixed Angle of Incidence ellipsometry measurements for Glass	15
4.2	Fixed Angle of Incidence ellipsometry measurements for Glass taken with a Neutral Density filter	15
4.3	Fixed Angle of Incidence ellipsometry measurements for a thick gold layer on Mica	16
4.4	Fixed Angle of Incidence ellipsometry measurements for a thin gold layer on glass.	17
4.5	Fixed Angle of Incidence ellipsometry measurements for a thick gold film on glass.	17
4.6	Fixed Angle of Incidence ellipsometry measurements for a gold film on Silicon	18
4.7	Fixed Angle of Incidence ellipsometry measurements for a silicon wafer	18
4.8	Variable angle of incidence measurements for a silicon wafer.	19
4.9	Variable angle of incidence measurements for a thin gold film on glass.	20
4.10	Variable wavelength ellipsometry measurements for a thin gold film on glass taken with a commercial ellipsometer.	21
4.11	Variable wavelength ellipsometry measurements for a silicon wafer taken with a commercial ellipsometer.	21

List of Tables

3.1	List of all the 3D printed Ellipsometer Parts with the time taken for their print and their corresponding weight in PLA(with a price of approximately 3 cents per gram).	11
5.1	Summary of results obtained from Fixed Angle of Incidence measurements using the 3D printed ellipsometer.	22
5.2	Summary of results obtained from Fixed Angle of Incidence measurements using the 3D printed ellipsometer.	22

Contents

List of Figures	ii
List of Tables	ii
1 Introduction and Background	1
1.1 Ellipsometry	1
1.2 3D Printing	1
1.3 Literature Review	2
1.4 Aims and Objectives	2
2 Ellipsometry Theory	3
2.1 Rotating Angular Ellipsometry	3
2.2 Fixed Angle of Incidence Ellipsometry	7
3 Experimental Methods	8
3.1 Overview of The 3D printed Ellipsometer	8
3.2 Preparation of the CAD files for 3D printing	10
3.3 Determining the p and s orientations of the Polarisers	10
3.4 Calibration of the Detector	12
3.5 Creating the Thin Gold Film Sample	14
4 Results	14
4.1 Fixed Incident Angle Ellipsometry	14
4.1.1 Two Interface Mediums	14
4.1.2 Three Interface Mediums	16
4.2 Variable Angle of Incidence Measurements	19
4.3 A note on Instrument Errors	20
4.4 Commercial Ellipsometer Measurements	20
5 Discussion	22
5.1 Factors Effecting Measurements	23
6 Conclusion	23
7 References	24
8 Appendices	26
8.1 Appendix 1: Risk Assessment	26
8.2 Appendix 2: Python Scripts	28

1 Introduction and Background

1.1 Ellipsometry

Ellipsometry is a nondestructive optical technique used to measure the thickness and optical properties of thin films and surfaces, the technique was first used in the late 1800s [5] though at that point not yet called ellipsometry. The technique is based on the analysis of polarization changes of light reflected or transmitted by a sample surface. When polarised light is incident on the surface, the reflected or transmitted light will change its polarisation state due to its interaction with the sample. Ellipsometry measures this change in polarisation state and can from this measurement determine various optical properties of the material. Readings obtained from ellipsometry can provide information about the physical structure, chemical composition, and optical properties of a sample. This information can be used to determine parameters such as film thickness, refractive index, the presence of surface coatings and impurities. Ellipsometry is widely used in materials science, surface science, semiconductor technology, and the development of new materials and devices, and is particularly useful in that it is unobtrusive, allowing measurements to take place *in situ* [3] without damaging the samples.

1.2 3D Printing

3D printing technology, also known as additive manufacturing, is a process of creating three-dimensional objects by adding material layer by layer. This technology has revolutionised the process of designing, prototyping, and manufacturing products, allowing for greater customization, faster prototyping, and more efficient production[6].

The basic process of 3D printing involves the creation of a 3D model using computer-aided design (CAD) software. The model is then sliced into thin layers, and the 3D printer builds the object by adding one layer at a time. The material used for printing can vary depending on the printer, but commonly some type of thermoplastic, although metals can be used too.

Fused Deposition Modelling (FDM) is the process that was used in this project, it is one of the most common types of 3D printing. These printers use a thermoplastic filament that is melted and extruded through a nozzle. The nozzle moves over a platform, depositing the material layer by layer to create the object.

The technology is very new and still rapidly developing, leading to an ever increasing accuracy and affordability. Due to these facts it is becoming more and more widespread in third level institutions. There is still however relatively few cases of research utilising 3D printing in physics[7]. Of all the sciences, Chemistry has probably made the most use of this powerful tool so far[8][9][10][11]. 3D printing is of particular interest in optical physics, where the price for optical components and the lack of engineering standards is “often a barrier for research”[12]. The customizability and affordability of 3D printing could overcome these hurdles, and there are already several examples of this in the field [13][14][12].

1.3 Literature Review

The inspiration for this thesis was the journal article “Optical measurements on a budget: A 3D-printed ellipsometer”[4]. Which is a paper detailing the design, fabrication and operation of a 3D-printed ellipsometer, with the intent to reduce the barrier for entry for the use of ellipsometry by undergraduates. The paper covers basic ellipsometric theory, details the design and fabrication process of the ellipsometer, provides a model fitting Excel sheet, and finally goes on to compare the performance of the printed instrument with commercial alternatives.

“Ellipsometry and Polarized Light”[3] is a comprehensive book that provides an in-depth guide to the theory and applications of ellipsometry. The book covers the basic principles of ellipsometry, including the polarisation of light and the Fresnel equations, and goes on to discuss the various different forms of the technique, such as thin film ellipsometry, film free ellipsometry, variable and fixed angle and variable and fixed wavelength ellipsometry.

A User’s Guide to Ellipsometry[2] is written specifically for users who are new to the technique. The book provides a practical introduction to ellipsometry, covering the basic principles, instrumentation, and data analysis techniques. The book also includes a section on sample preparation and measurement procedures, as well as several case studies that demonstrate the application of ellipsometry to various materials and surfaces.

1.4 Aims and Objectives

The primary aim of this thesis is to produce a working 3D-printed ellipsometer based on the paper “Optical measurements on a budget: A 3D-printed ellipsometer”[4] that can be used to obtain the optical constants of a variety of surfaces and thin films. The ellipsometer design will be modified as required and fabricated using a 3D printer and will be tested and compared to a commercial instrument to determine its performance.

To achieve the above aim, the following objectives will be pursued:

Adapt the ellipsometer design used in the paper[4], to fit our equipment.

Fabricate the 3D-printed ellipsometer using a 3D printer and assemble it with the necessary components and software.

Fabricate sample thin films for testing using evaporation deposition.

Calibrate all components of the ellipsometer and take some simple readings to ensure it is working as intended.

Take fixed angle of incidence readings with the ellipsometer for a range of samples and use these to calculate the refractive index of the samples.

Take variable angle of incidence readings for a range of samples and use these to calculate both the refractive index and film thickness of the samples.

Take Measurements of the samples using a commercial ellipsometer, and compare these readings to the ones taken with the 3D printed instrument.

Overall, the thesis aims to demonstrate the potential of 3D printing technology in the design and fabrication of scientific instruments, specifically ellipsometers, and its use in the analysis of surfaces and thin films.

2 Ellipsometry Theory

When light hits a surface, the state of polarisation of the light can change via reflection, refraction, transmission, or scattering. Measurement of this change in polarisation is known as ellipsometry[3] and can yield the optical properties of the material. This paper will focus on the change of state of polarisation due to reflection/refraction.

2.1 Rotating Angular Ellipsometry

We will begin by discussing the theory utilised in rotating angular ellipsometry(RAE) where the polariser angle is fixed and multiple analyser angle intensities are measured as a function of angle of incidence. Lets begin with our description of light incident on a material \tilde{N}_3 with thin film \tilde{N}_2 of thickness d shown in Fig 2.1. Where \tilde{N} is the complex index of refraction for the different layers. \tilde{N} is composed of the usual real index of refraction n and the so called Gauchy Extinction coefficient k which is complex. In the case of dielectrics k is zero, and we have the usual index of refraction. This interaction

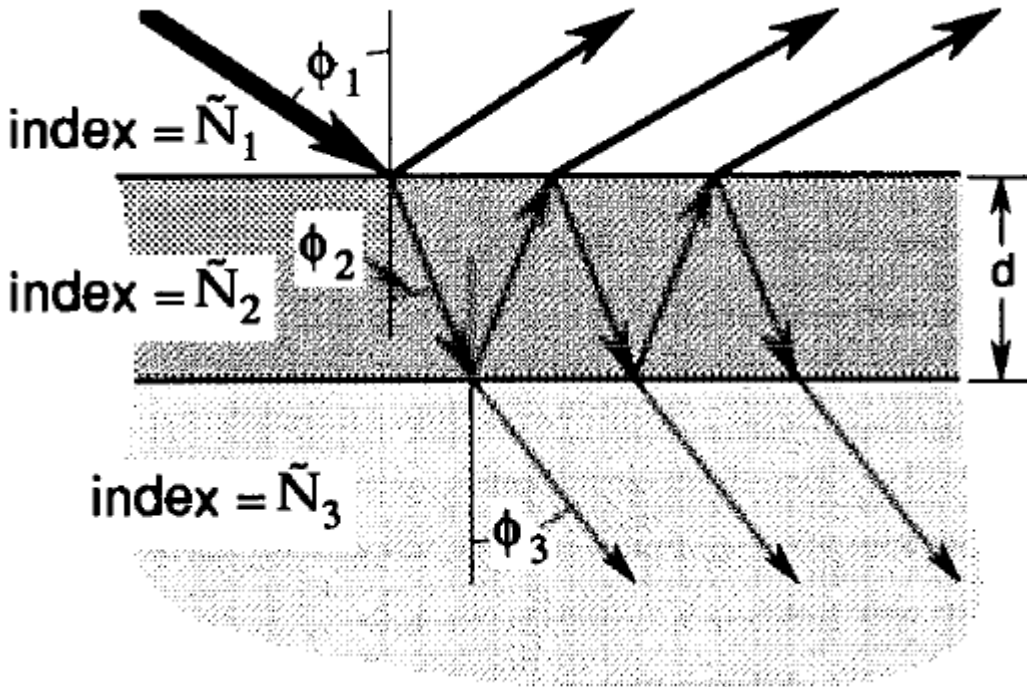


Figure 2.1: Light incident on a thin film of thickness d .[2]

with the thin film can be described using reflection coefficients which are the ratio of the incident to reflected light amplitudes and are given by Eq(2.3). Where p and s denote parallel and perpendicular polarised incident light, r are the fresnel reflection coefficients for the different interfaces and β is the film phase thickness, as shown below.

$$r_p = \frac{\tilde{N}_2 \cos(\phi_1) - \tilde{N}_1 \cos(\phi_2)}{\tilde{N}_2 \cos(\phi_1) + \tilde{N}_1 \cos(\phi_2)} \quad (2.1)$$

$$r_s = \frac{\tilde{N}_1 \cos(\phi_1) - \tilde{N}_2 \cos(\phi_2)}{\tilde{N}_1 \cos(\phi_1) + \tilde{N}_2 \cos(\phi_2)} \quad (2.2)$$

$$R^{p,s} = \frac{r_{12}^{p,s} + r_{23}^{p,s} e^{-i2\beta}}{1 + r_{12}^{p,s} r_{23}^{p,s} e^{-i2\beta}} \quad (2.3)$$

$$\beta = 2\pi \left(\frac{d}{\lambda} \right) \tilde{N}_2 \cos(\phi_2) \quad (2.4)$$

In ellipsometry we will be measuring light intensities which are proportional to the square of the amplitudes and therefore term we will use the Reflectance \mathcal{R} which is given below.

$$\mathcal{R}^{p,s} = |R^{p,s}|^2 \quad (2.5)$$

Having established this we can now introduce the two parameters which are of primary interest in ellipsometry and these are Δ and Ψ , dubbed the Ellipsometry angles[3]. The equation for Ψ and Δ is given below. δ_p and δ_s are the phase shift upon reflection again for parallel and perpendicularly polarised incident light.

$$\tan(\Psi) = \frac{|R_p|}{|R_s|} \quad (2.6)$$

$$\Delta = \delta_p - \delta_s \quad (2.7)$$

From the above equations we get what is known as the Fundamental Equation of Ellipsometry[2] which describes ρ the complex ratio of the total reflection co-efficients in terms of Ψ and Δ .

$$\rho = \tan(\psi) e^{i\Delta} = \frac{R_p}{R_s} Eq6 \quad (2.8)$$

The ellipsometry angles vary with angle of incidence(AoI), film thickness and film refractive index, so for RAE each incident angle will have different ellipsometry angles. The theoretical plots for ellipsometry angles vs incident angles for a thick (Fig 2.2) and thin (Fig 2.3) gold film are given below. Where the thick film is considered thick enough to be a two medium interface.

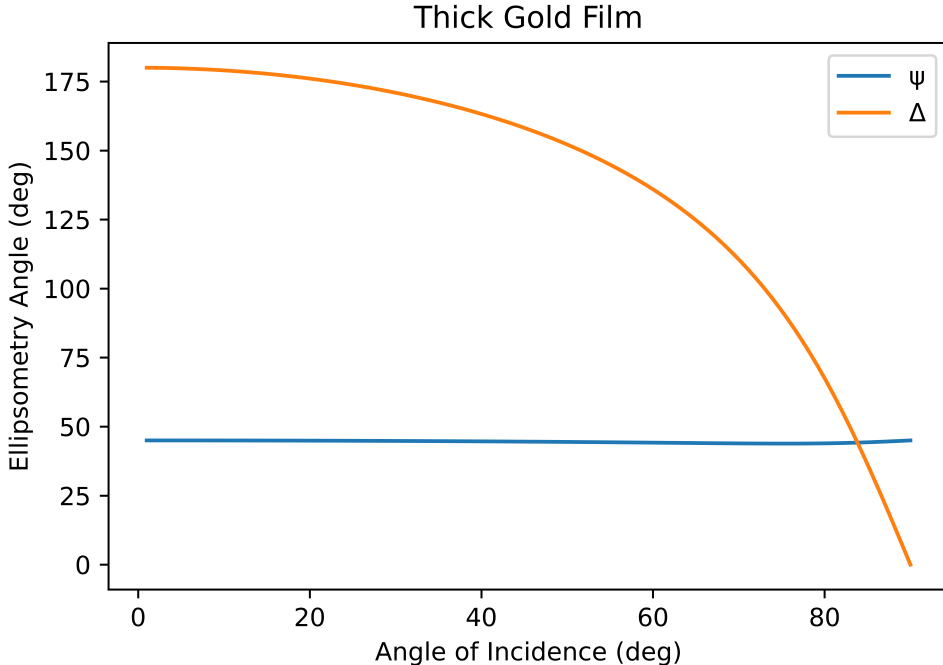


Figure 2.2: Theoretical plot of Ellipsometry Angles vs AoI for a thick gold film at a wavelength of 650nm and $\tilde{N}_{Au} = 0.1556 + 3.6i$.

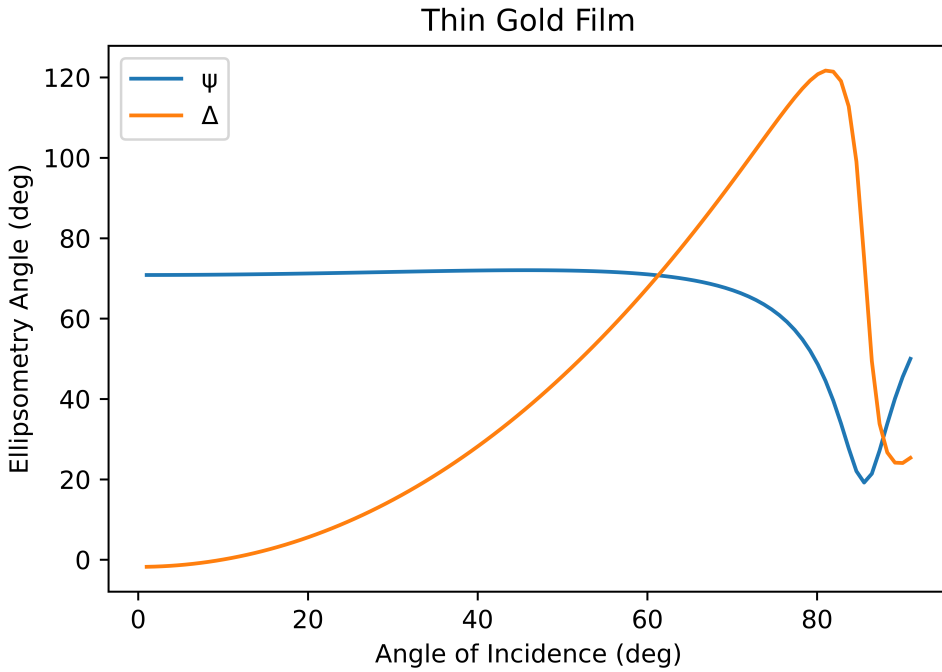


Figure 2.3: Theoretical plot of Ellipsometry Angles vs AoI for a thin gold film(10nm) at a wavelength of 650nm and $\tilde{N}_{Au} = 0.1556 + 3.6i$.

Once the ellipsometry angles are found as a function of Angle of Incidence, we can graph that and also graph the theoretical values of Ψ and Δ for a range of \tilde{N} and film thickness d . Then using a least squares approach we can narrow down the values for \tilde{N} and d that best fit our data. If one of the two values (\tilde{N} and d) are already known we can fix the known parameter in our model and only need to vary the unknown parameter.

We will discuss below the process for obtaining Δ and Ψ

A general setup for ellipsometry is given in Fig 2.4. Where we have the light source L , in our case a monochromatic source, followed by a polariser P then the sample in question S followed by another polariser known as the analyser A and finally a detector D . Utilising the combination of P and A we can determine the change in polarisation of the light due to the interaction with the sample. The incident light will change in polarisation in two main ways, firstly via the change in phase due to the interference of different reflected waves and secondly via the an-isotropic reflection of the polarised light depending on its initial state of polarisation.

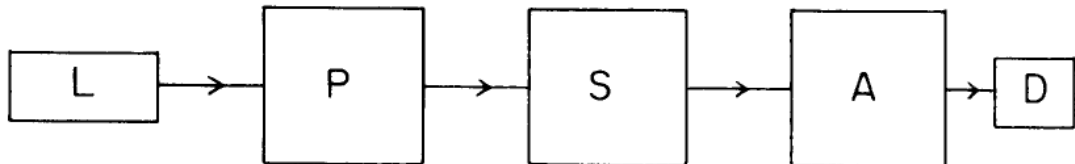


Figure 2.4: Basic diagram of the components of an ellipsometer[3].

The Stokes parameters are used to describe the state of polarisation of light, they can also be used to describe partially or un-polarised light[15].They are our preferred

method for describing the polarised state of light because they relate to the intensities of the light which are directly measurable. The Stokes Parameters can be combined into a 4-dimensional vector known as the Stokes Vector and is given below[16] where $I_{0^\circ}, I_{45^\circ}, I_{90^\circ}, I_{-45^\circ}, I_R$ and I_L are the measured light intensities of light having passed through a linear polariser A at $0^\circ, 45^\circ, 90^\circ, -45^\circ$ and a Left and Right circular polariser respectively. Thus a measurement of these six quantities will provide you with the stokes vector, however simplifications can be made in order to reduce the number of required measurements We can use Eq(2.10) to eliminate the need to measure one parameter.

$$S = \begin{pmatrix} S_0 \\ S_1 \\ S_2 \\ S_3 \end{pmatrix} = \begin{pmatrix} I_{0^\circ} + I_{90^\circ} \\ I_{0^\circ} - I_{90^\circ} \\ I_{45^\circ} - I_{-45^\circ} \\ I_R - I_L \end{pmatrix} \quad (2.9)$$

$$S_0^2 = S_1^2 + S_2^2 + S_3^2 \quad (2.10)$$

$$S_0 = I_{0^\circ} + I_{90^\circ} = I_{45^\circ} + I_{-45^\circ} = I_R + I_L \quad (2.11)$$

Using the above equations we get the following four equations relating intensity of light having passed through various angles of our analyser A to the stokes parameters[4].

$$I_{0^\circ} = \frac{1}{2}(S_0 + S_1) \quad (2.12)$$

$$I_{45^\circ} = \frac{1}{2}(S_0 + S_2) \quad (2.13)$$

$$I_{90^\circ} = \frac{1}{2}(S_0 - S_1) \quad (2.14)$$

$$I_{-45^\circ} = \frac{1}{2}(S_0 - S_2) \quad (2.15)$$

These are specific solutions to the general equation given below. Where θ_A is the angle of the analyser A .

$$I(\theta_A) = \frac{1}{2}[S_0 + S_1\text{Cos}(2\theta_A) + S_2\text{Sin}(2\theta_A)] \quad (2.16)$$

The stokes parameters relate to Δ and Ψ by the following equations where θ_P is the angle of the polariser P .

$$\Psi = \text{Tan}^{-1}\left(\text{Tan}(\theta_P) \times \text{Tan}\left(\frac{\text{Cos}^{-1}(-\frac{S_1}{S_0})}{2}\right)\right) \quad (2.17)$$

$$\Delta = \text{Cos}^{-1}\left(\frac{\frac{S_2}{S_0}}{\text{Sin}\left(2 \times \text{Tan}^{-1}\left(\frac{\text{Tan}(\Psi)}{\text{Tan}(\theta_P)}\right)\right)}\right) \quad (2.18)$$

2.2 Fixed Angle of Incidence Ellipsometry

An alternative method utilises a fixed angle of incidence and measures the intensity as a function of analyser angle, again with a fixed polariser angle to determine both \tilde{N} and d . Where the intensity is given by Eq(2.16), in this case the ellipsometry angles will be the same for all measurements. From the measurements of intensity vs AoI values for the Stokes parameters can be calculated using Eq(2.16). Then using Eq(2.19) and (2.20) values for Ψ' and Δ can be determined where Ψ' is given by Eq(2.21).

$$\cos(2\Psi') = -\frac{S_1}{S_0} \quad (2.19)$$

$$\sin(2\Psi')\cos(\Delta) = \frac{S_2}{S_0} \quad (2.20)$$

$$\tan(\Psi') = \frac{\tan(\Psi)}{\tan(\theta_P)} \quad (2.21)$$

Using the Fresnel reflection coefficients where ϕ_2 is given by Eq(2.22)(snell's law) \tilde{N}_2 can be calculated.

$$\cos(\phi_2) = \sqrt{1 - \left(\frac{\tilde{N}_1}{\tilde{N}_2}\right)^2 \sin^2(\phi_1)} \quad (2.22)$$

$$\tilde{N}_2 = \frac{\left[\sqrt{1 - 4\sin^2(\phi_1)\tan(\Psi)e^{i\Delta} + 2\tan(\Psi)e^{i\Delta} + \tan^2(\Psi)e^{i\Delta}} \right] \tilde{N}_1 \sin(\phi_1)}{\cos(\phi_1) [1 + \tan(\Psi)e^{i\Delta}]} \quad (2.23)$$

Solving for film thickness. Starting from Eq(2.8) we can plug in the values for the reflectance of Eq(2.1), giving the below equation.

$$\rho = \frac{r_{12}^p + r_{23}^p e^{-i2\beta}}{1 + r_{12}^p r_{23}^p e^{-i2\beta}} \times \frac{1 + r_{12}^s r_{23}^s e^{-i2\beta}}{r_{12}^s + r_{23}^s e^{-i2\beta}} \quad (2.24)$$

We can rewrite this using ρ as

$$\rho = \frac{AX^2 + BX + C}{DX^2 + EX + F} \quad (2.25)$$

where

$$A = r_{23}^p r_{12}^s r_{23}^s \quad (2.26)$$

$$B = r_{12}^p r_{12}^s r_{23}^s + r_{23}^p \quad (2.27)$$

$$C = r_{12}^p \quad (2.28)$$

$$D = r_{23}^s r_{12}^p r_{23}^p \quad (2.29)$$

$$E = r_{12}^s r_{12}^p r_{23}^p + r_{23}^s \quad (2.30)$$

$$F = r_{12}^s \quad (2.31)$$

$$X = e^{-i2\beta} \quad (2.32)$$

Solving this for X we get

$$X = \frac{(-\rho E - B) \pm \sqrt{(\rho E - B)^2 - 4(\rho D - A)(\rho F - C)}}{2(\rho D - A)} \quad (2.33)$$

It is now possible to solve this for X , either by iteration if \tilde{N}_2 is unknown and real, using the fact that $|X| = 1$ or if \tilde{N}_2 is known simply by solving the above equation. With this value for X we can now determine d the film thickness by the following procedure.

Subbing $X = e^{-i2\beta}$ into Eq(2.24) we get

$$e^{-i2\beta} = \frac{(-\rho E - B) \pm \sqrt{(\rho E - B)^2 - 4(\rho D - A)(\rho F - C)}}{2(\rho D - A)} \quad (2.34)$$

Since β depends on the film thickness by Eq(2.4) we can solve this for d

$$\ln(X) = -i4\pi \frac{d}{\lambda} \tilde{N}_2 \cos(\theta_2) \quad (2.35)$$

And Solving for the film thickness d we get.

$$d = \frac{i(\ln(X)\lambda)}{4\pi \tilde{N}_2 \cos(\phi_2)} \quad (2.36)$$

Seeing as there are two solutions to Eq(2.33) this will provide two values for d . Complex thickness are meaningless however so we choose the real solution.

3 Experimental Methods

3.1 Overview of The 3D printed Ellipsometer

The Design of the ellipsometer we will be using is a Rotating Angular Ellipsometer. In this setup the analyser angle θ_A will be set for a range of incident angles θ_i and the corresponding light intensities will be measured. The analyser angle will typically be set at 4 different angles ($0^\circ, 45^\circ, 90^\circ, -45^\circ$) and the Polariser angle θ_P will be fixed at 45° . Figure(3.1) shows the main goniometer assembly for the 3D printed Ellipsometer. This consists of two goinometer arms that are attached to the Goniometer body D via a hinge pin, they are also attached to the circular rail system B via two screws. The arms are able to rotate for an angle of incidence from 0° to 90° though in practise we are limited to about 15° to 65° due to the optical mounts interfering with each other. This whole system is attached to a standard optic bench via the countersunk holes E. The two arms have a rail mount system C for the mounting of the other optical components, namely the Laser mount, the Detector mount and the two polariser mounts. The angle of incidence is measured using the pointers A at the ends of both arms. There are several factors which are important in this assembly. Firstly all the optical components must be on the same level, this is where the circular rail system comes in allowing you to firmly attach the goniometer arms to the main body removing the risk of one arm being skewed in relation to the other, secondly the hinge point of the whole system needs to be clear so that the Sample mount can correctly be positioned above this.

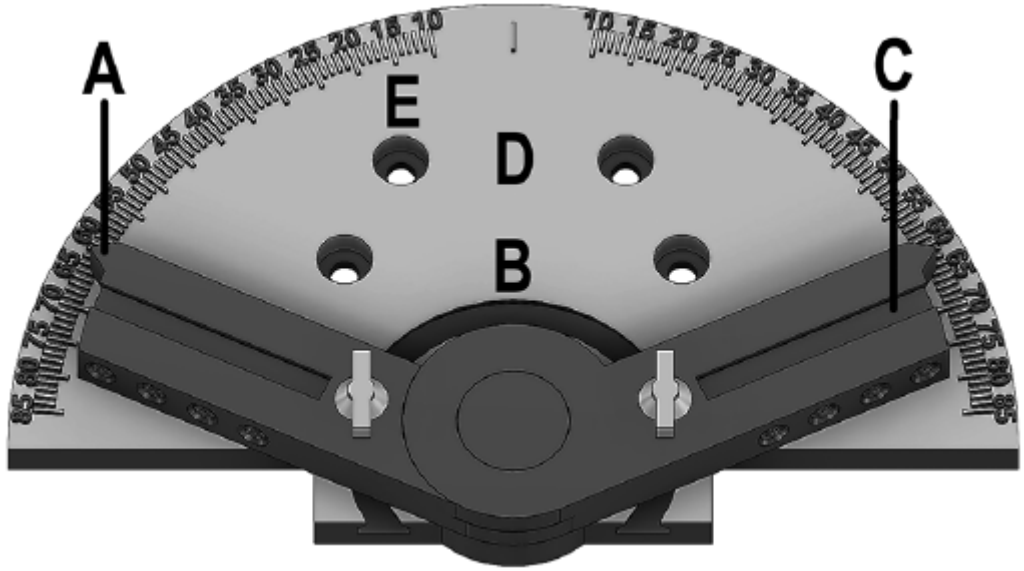


Figure 3.1: CAD model of the two goinometer arms attached to the main body of the ellipsometer[4].

Figure 3.2 shows the Sample mount for the Ellipsometer. Consisting of the sample mount base A which screws into a standard optical bench, an adjustment screw B which can be turned to adjust the linear position of the sample mount C so as to align our sample with the centre of the optical axis. The sample is held in place with the simple clamping device D.

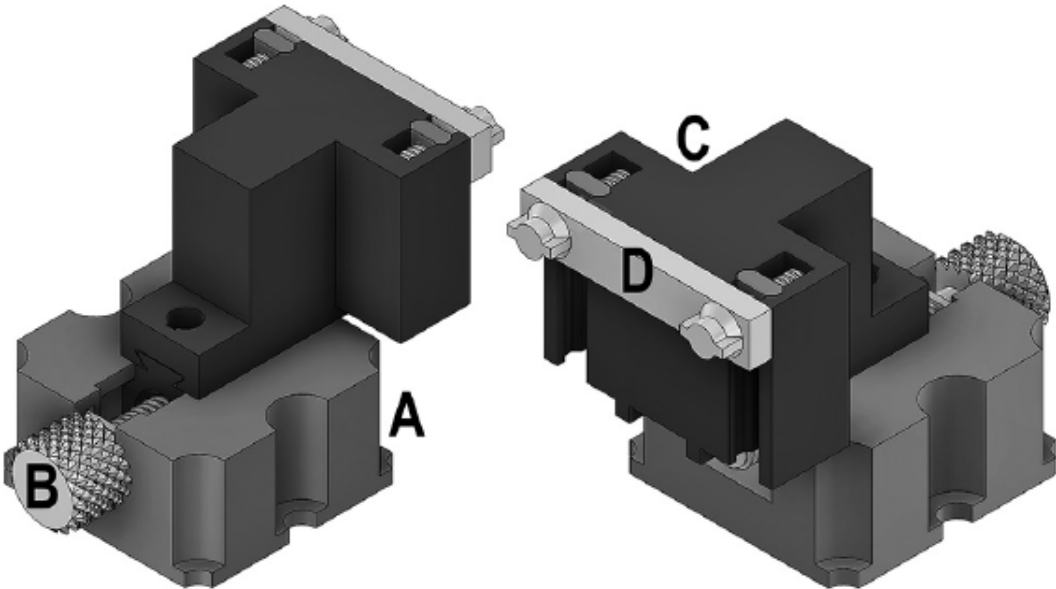


Figure 3.2: CAD model of the ellipsometer sample mount[4].

The polariser mounts shown in Figure 3.3 are rotated using a wormdrive A with a 42:1 ratio. Allowing incremental changes in polariser angle to be easily achievable. The polarisers are held in place at C with a screw cap.

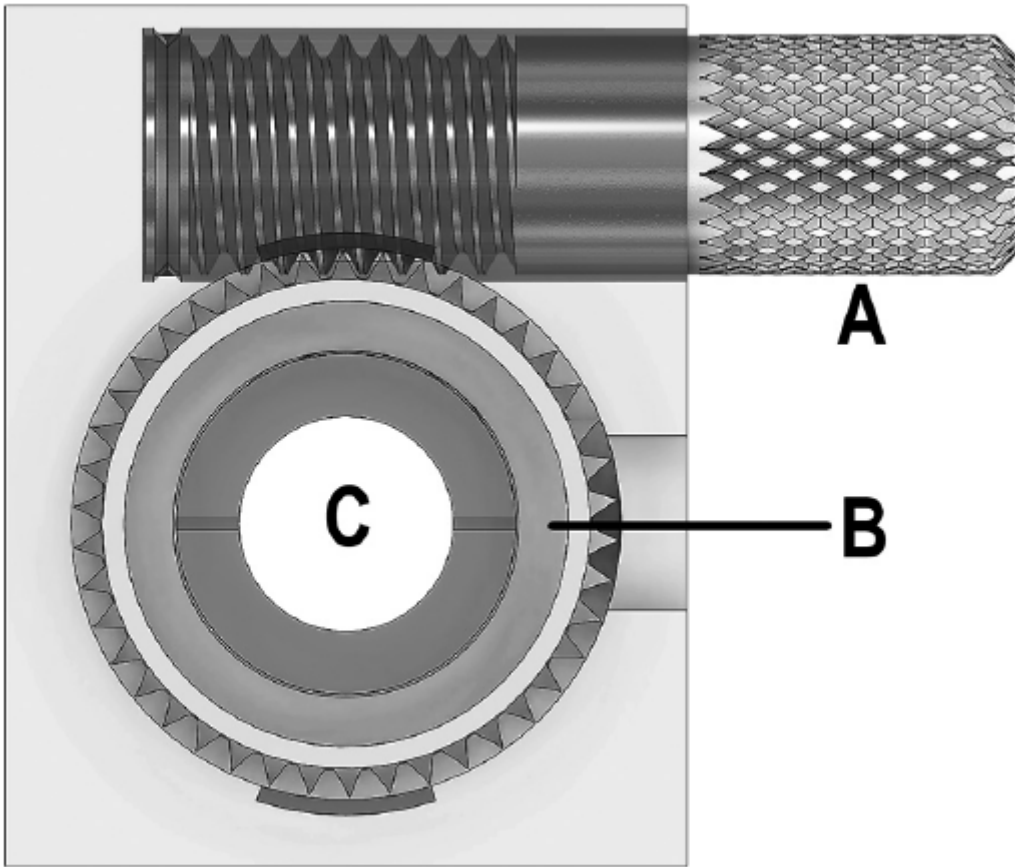


Figure 3.3: CAD model of the ellipsometer polariser mount with the worm drive.

3.2 Preparation of the CAD files for 3D printing

The first step of the process in constructing the ellipsometer was the preparation of the CAD files. The bulk of the files could remain unchanged from the source files, however both the laser mount and detector mount both had to be adapted to house the laser and detector we would be using. This was a straightforward enough procedure wherein the files were brought in and modified in the open source programme FreeCad. Once all files were assembled in the .stl format they needed to be sliced. Slicing is the process by which a CAD file is deconstructed into a set of instructions for the 3D printer, giving it a path to follow and deposit its filament for each layer of the model. This is also the step where supports are added to the CAD file to allow the printer to print overhanging sections. These supports are printed in such a way as to be easily removable upon completion of the print, there are also 3D printers with the capacity to print using multiple filaments at a time allowing you to print the supports from a water soluble material and dissolve them once the print is finished. In our case however an Ultimaker 2+ was used and so only a single filament could be printed at a time. The entire ellipsometer was printed in polylactic acid.

3.3 Determining the p and s orientations of the Polarisers

To determine the perpendicular (s) and parallel (p) polarisation states of the polarisers in the Ellipsometer, the Brewster's angle was used. The Brewster's angle (θ_B) is an angle

Table 3.1: List of all the 3D printed Ellipsometer Parts with the time taken for their print and their corresponding weight in PLA (with a price of approximately 3 cents per gram).

Part Name	Quantity	PLA Weight	Time for Print
Goniometer Arm (Left)	1	42	6h 53m
Goniometer Arm (Right)	1	42	6h 53m
Goniometer Hinge Pin	1	14	2h
Goniometer Body	1	240	37h 34m
Goniometer Rail Screw	2	2	40m
Goniometer Rail	2	0.12	10m
Linear Sample Mount Bar	2	6	1h 8m
Linear Sample Mount Body	1	54	8h 21m
Linear Sample Mount Drive	1	7	1h 20m
Linear Sample Mount Head	1	49	7h 31m
Linear Sample Mount Nut	4	0.2	16m
Linear Sample Mount Rail	1	5	57m
Linear Sample Mount Screw	4	4	1h 8m
Rotating Polariser Mount Body (Left)	1	15	2h 55m
Rotating Polariser Mount Body (Right)	1	15	2h 55m
Rotating Polariser Mount Cap	2	4	36m
Rotating Polariser Mount Gear-Optic Mount	2	6	1h 10m
Rotating Polariser Mount Optic Screw	2	2	20m
Rotating Polariser Mount Worm Drive	2	8	1h 26m
Laser Mount	1	10	1h 46m
Detector Mount	1	11	1h 55m
Total		536.32	87h 54m

of incidence for a given interface for which all the reflected light is polarised perpendicular to the plane of incidence (s-polarised) and is given by Eq(3.1). Using a glass slide as our sample and inserting one of the polarisers between the sample and the detector at an angle of incidence of θ_B , the polariser can be rotated until a minimum light intensity is achieved. This corresponds to the polariser being p-polarised. It is a good idea once this minimum is recorded to adjust the incident angle marginally until you are satisfied that a minimum is detected and you are at the correct value for θ_B . The polariser can then be turned until a maximum intensity is recorded, this occurs when the polariser is s-polarised. Repeating this for both polarisers it is straightforward to determine their angles. A check can be conducted on conclusion of this by aligning the polarisers at s and p polarisation states and ensuring that this records a minimum light intensity.

$$\theta_B = \tan^{-1} \left(\frac{N_1}{N_2} \right) \quad (3.1)$$

3.4 Calibration of the Detector

For this project it was decided to use an inexpensive silicone photodiode(BPW 21) in conjunction with a picoscope 200a as the detector and small laser with a wavelength of 650nm and operating voltage of 5v. To ensure the detector was behaving linearly. A set of measurements were taken for the laser light shone through two polarisers, and the Intensity was measured as a function of polariser angle. The Intensity of light Transmitted through two polarisers given a relative angle between them of θ is given by Eq(3.2), where I_t is the transmitted intensity and I_0 is the incident intensity.

$$I_t = I_0 \cos^2(\theta) \quad (3.2)$$

Figure 3.4 shows the raw data obtained. As is evident from the data the Detector is behaving as expected and a $\cos^2(\theta)$ is produced.

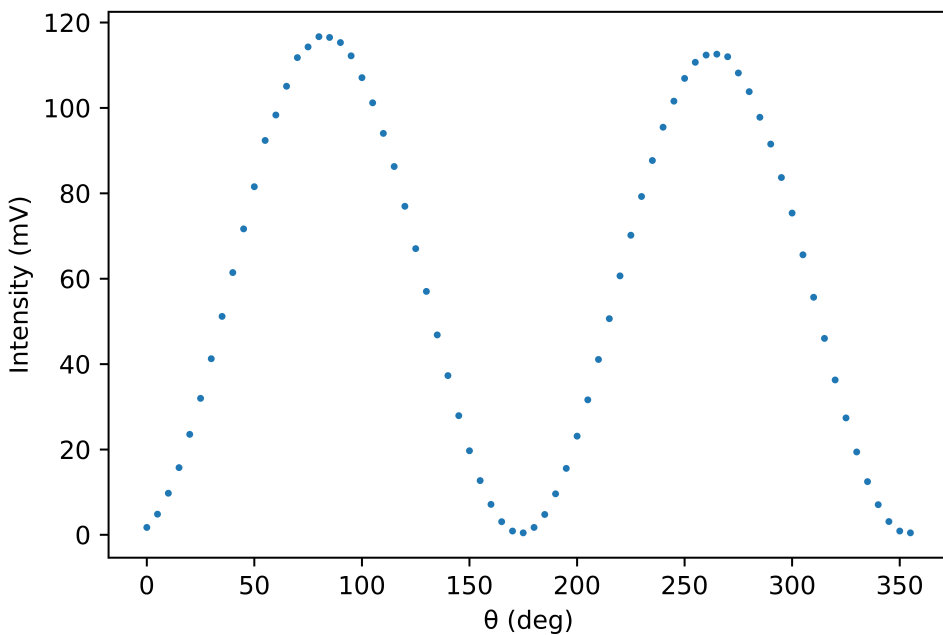


Figure 3.4: Laser calibration measurements of Intensity as a function of polariser angle.

To determine the linearity of the detector a plot of $\text{Cos}^2(\theta)$ vs the Intensity should provide a clear straight line, if the Intensity measurement is normalised, the line of best fit should have a slope of 1. The plot below (Fig 3.5) shows $\text{Cos}^2(\theta)$ vs the normalised intensity measurements along with the line of best fit, this line has a slope of 1.018, demonstrating the linearity of our detector.

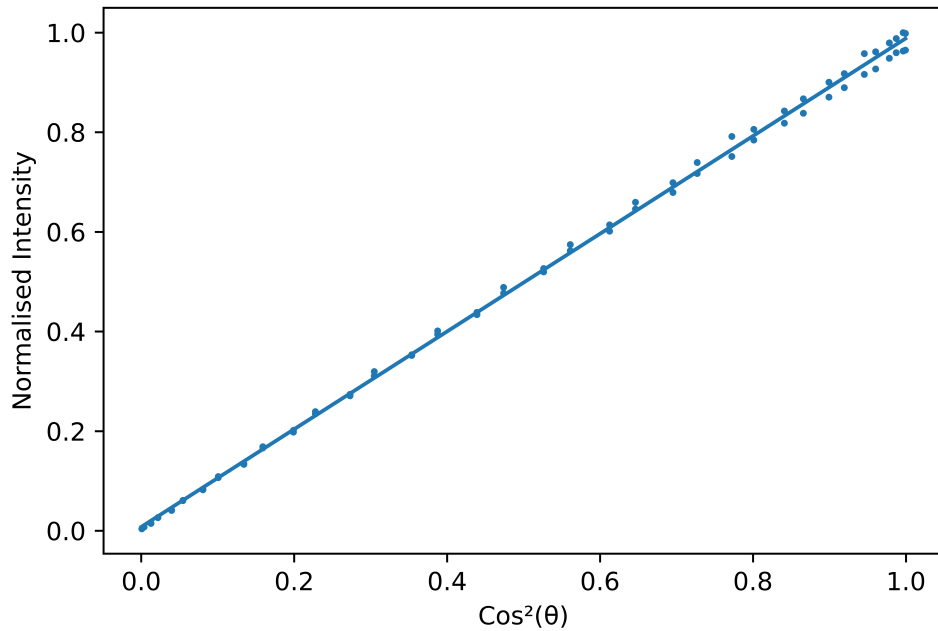


Figure 3.5: Plot of $\text{Cos}^2(\theta)$ vs Normalised Intensity with line of best fit.

3.5 Creating the Thin Gold Film Sample

On completion of the construction of the ellipsometer it remained to create a sample to test. Gold was our chosen thin film material as it doesn't react to create an oxide layer and hence change the refractive index of the thin film. The film was deposited onto the substrate(a glass slide) using a process known as Evaporation Deposition, whereby a crucible of metal is heated in a vacuum chamber until it begins to evaporate. This evaporated metal then condenses onto the substrate forming a thin film. The film thickness can be varied by varying the time the substrate is exposed to the evaporating metal. The film thickness can be calculated during deposition by using a crystal that is also exposed to the evaporating metal, as metal condenses on the crystal it changes its resonant frequency, this change can be measured and used to estimate the film thickness. In this way a glass slide with a thin gold film was created to test in the ellipsometer. In addition to this several other samples were obtained for testing, those being: a sample of gold deposited on mica, gold deposited on silicon and a silicon wafer with a thin silicon dioxide film.

4 Results

4.1 Fixed Incident Angle Ellipsometry

4.1.1 Two Interface Mediums

Measurements of Fixed Angle of Incidence were taken to begin with for a glass slide with no thin film. With the intent of determining the refractive index of Glass. For these measurements the incident angle and Polariser angle remained fixed for the entire experiment and the Analyser angle was rotated through 360 degrees. To accommodate incremental changes in the Analyser angle the screw was rotated in half turn increments providing a step size of 4.286 degrees.

The Angle of Incidence for these measurements was set at 45° and the Polariser angle to 45° . Figure 4.1 shows a Plot of the measurements for the glass slide along with the theoretical values. On inspection of this initial result it appears that the measured values are being flattened at high intensities. A possible explanation of this could be that the detector was being saturated at the higher intensities. To resolve this issue a neutral density filter was placed in the system after the laser to reduce the intensity of light incident on the detector. A filter was chosen such that it reduced the maximum intensity to below 200mV.

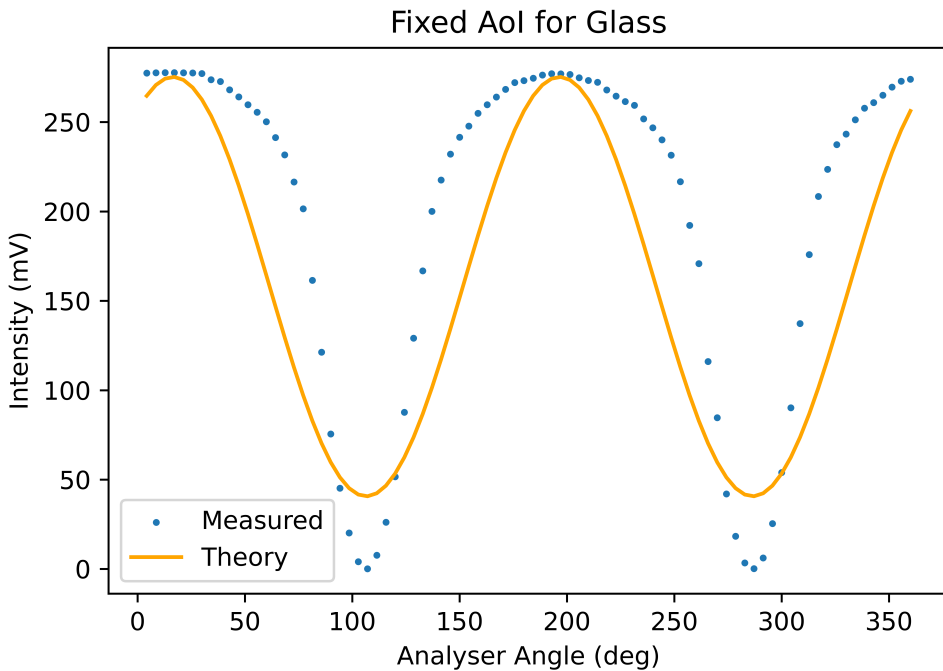


Figure 4.1: Fixed Angle of Incidence ellipsometry measurements for Glass

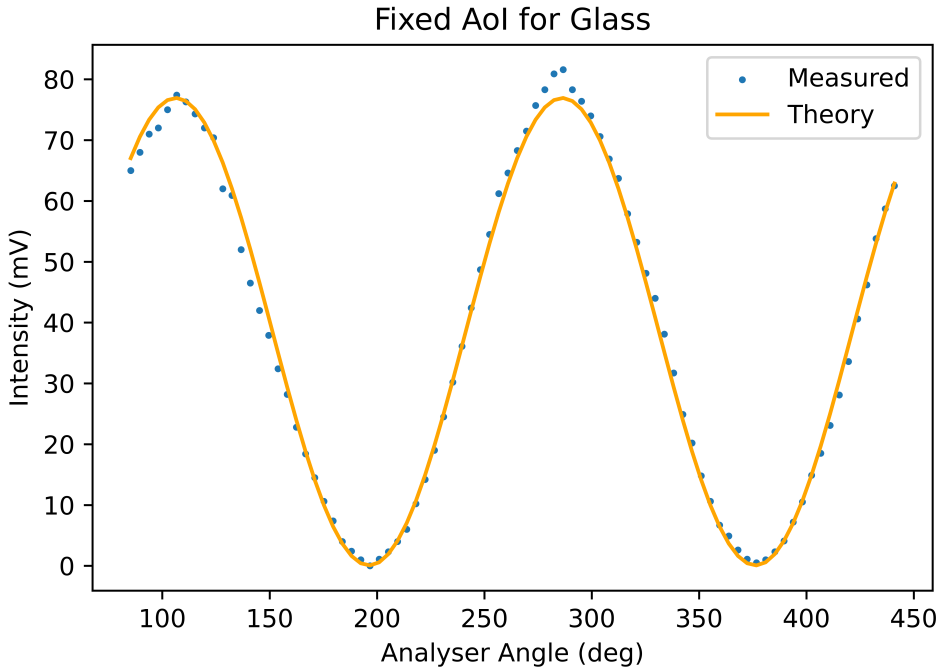


Figure 4.2: Fixed Angle of Incidence ellipsometry measurements for Glass taken with a Neutral Density filter

Figure 4.2 shows the new measurement set for glass along with the theoretical values. With the inclusion of the Neutral Density Filters the measured intensities now match the theoretical values. Calculating a value for the refractive index from this set of measure-

ments using the process outlined in the theory section we calculate $n_{glass} = 1.46 \pm .07$. Where the error is found by taking the standard error on the mean from a regression fit of $\text{Cos}(\theta_A)$ and $\text{Sin}(\theta_A)$ vs the measured intensity. This provides a value and an error for the Stokes parameters. Using these, values for the refractive index and there corresponding error was calculated.

The next sample that was measured was a gold layer on mica. The gold was suitably thick to consider only the interface between the gold and air. Fixed Angle of Incidence measurements were taken and are shown in Figure 4.3. Calculating a value for the refractive index of gold to be $\tilde{N}_{Au} = 0.26 \pm 0.04 + 3.310i \pm 0.2i$

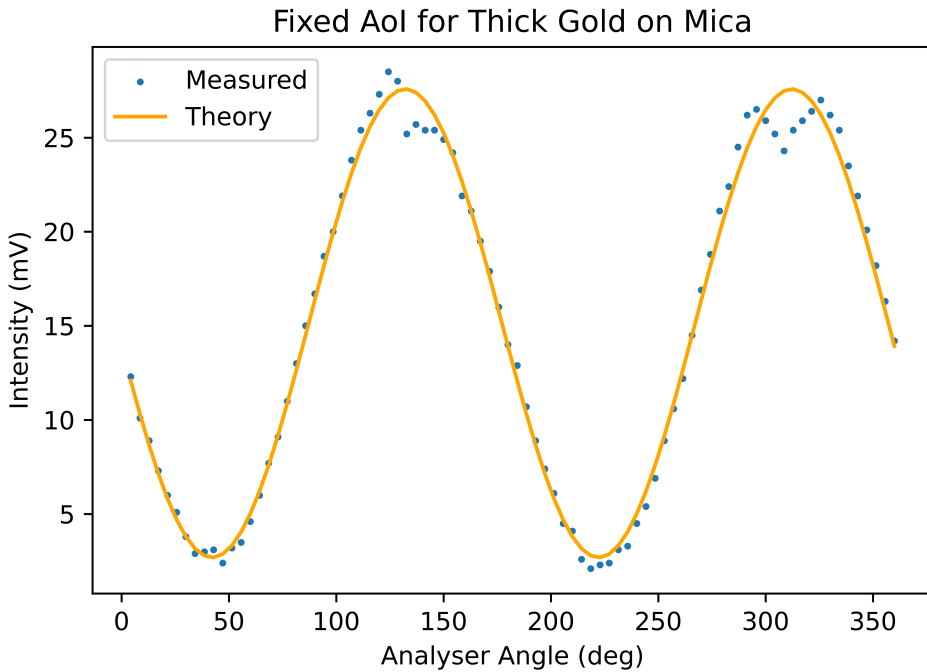


Figure 4.3: Fixed Angle of Incidence ellipsometry measurements for a thick gold layer on Mica

4.1.2 Three Interface Mediums

After taking several Fixed AoI measurements for a two interface medium, measurements for a three interface medium were taken. Beginning with a thin Gold Film deposited on glass. Figure 4.4 shows the values obtained as well as the theoretical values. Calculating the values for \tilde{N} for this sample we got $\tilde{N}_{Au} = 0.42 \pm 0.08 + 3.620i \pm 0.2i$

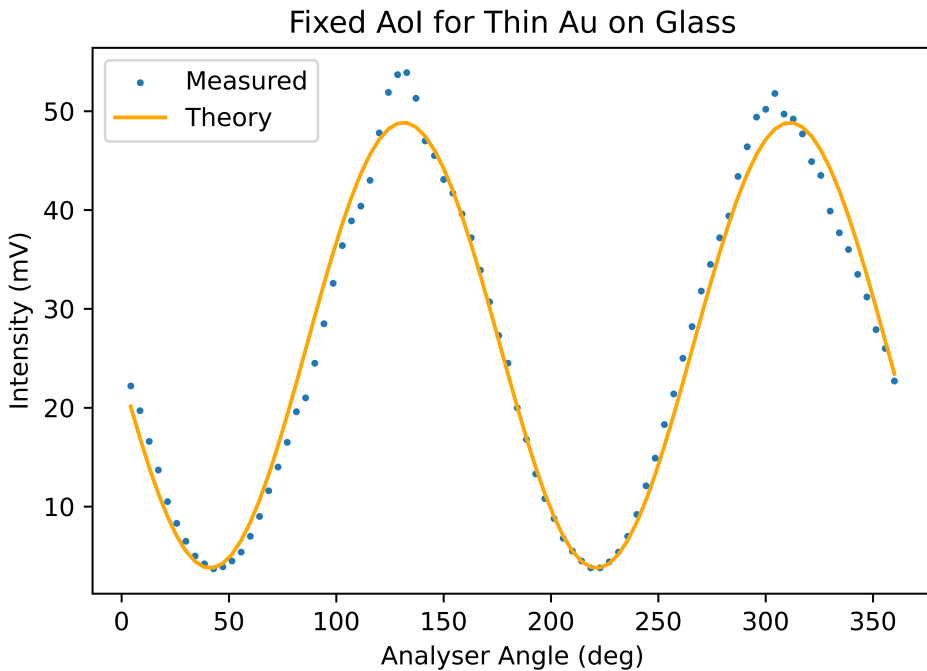


Figure 4.4: Fixed Angle of Incidence ellipsometry measurements for a thin gold layer on glass.

Then a sample consisting of a thicker gold layer on glass was tested (Fig 4.5) which produced a value for $\tilde{N}_{Au} = 0.52 \pm 0.07 + 3.15i \pm 0.1i$

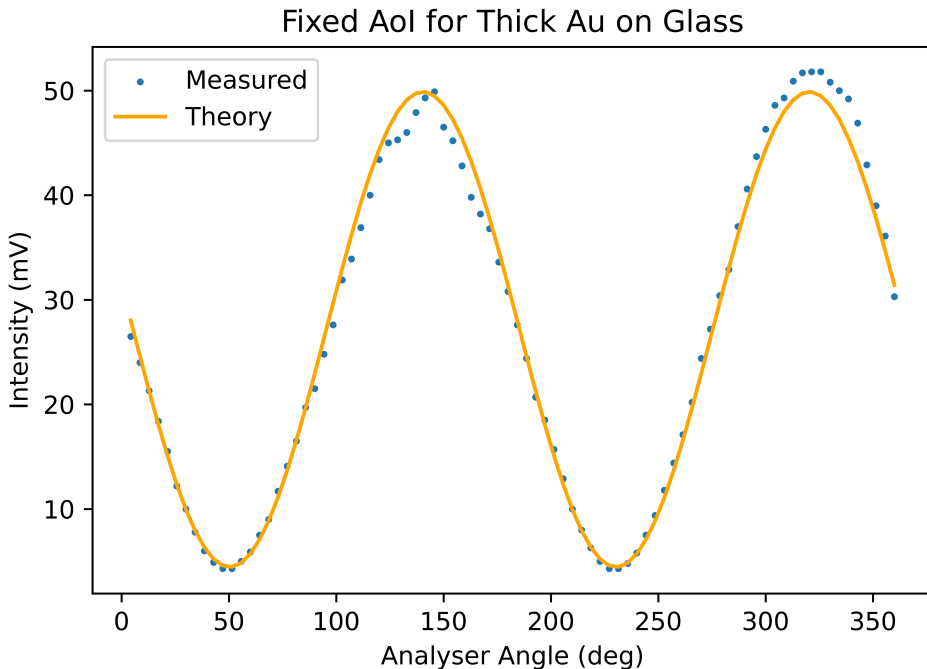


Figure 4.5: Fixed Angle of Incidence ellipsometry measurements for a thick gold film on glass.

Measurements were also taken for a sample of gold on a silicon wafer (Fig 4.6), this system actually also compromises of a very thin layer of Titanium between the gold and silicon to aid in an even deposit of gold. These measurements provided a value for $\tilde{N}_{Au} = 0.96 \pm 0.1 + 1.74i \pm 0.06i$.

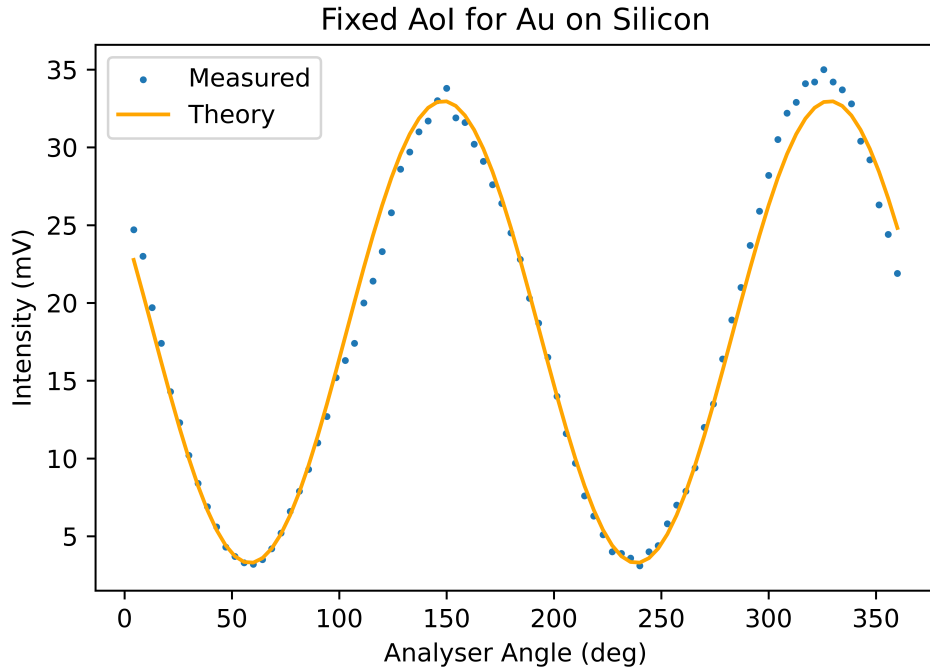


Figure 4.6: Fixed Angle of Incidence ellipsometry measurements for a gold film on Silicon

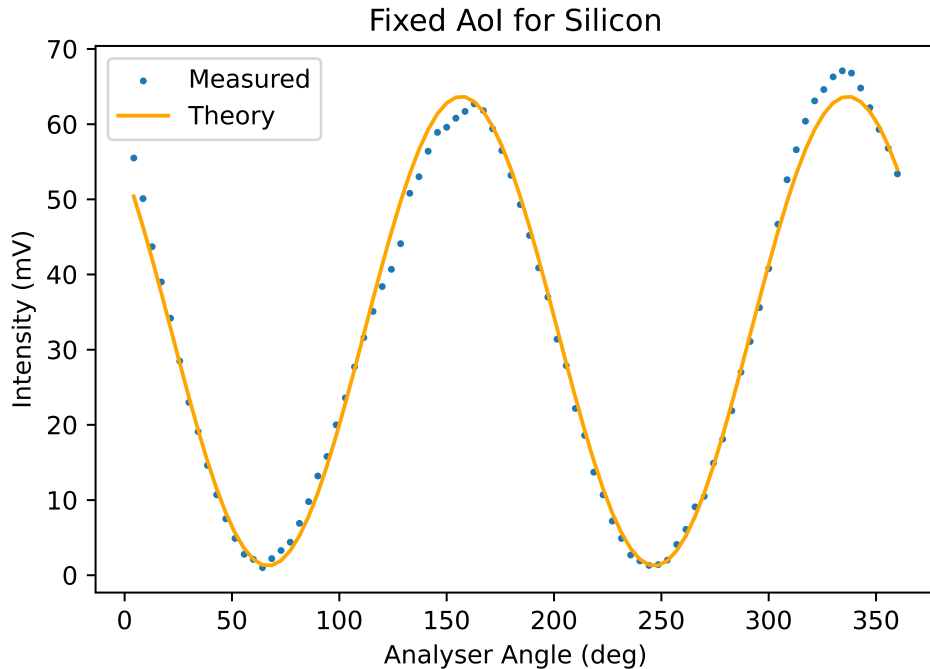


Figure 4.7: Fixed Angle of Incidence ellipsometry measurements for a silicon wafer

Finally measurements for the silicon wafer were taken (Fig 4.7). This sample consisted of pure silicon and then a thin silicon oxide layer. These measurements returned a value of $\tilde{N}_{SiO_2} = 1.68 \pm 0.1 + 0.44i \pm 0.2i$.

4.2 Variable Angle of Incidence Measurements

The next set of measurements were taken using a Variable Angle of Incidence, where several intensities were measured over a range of Angle of incidence, to create a plot of Ellipsometry angles over Incident Angle. The polariser was fixed at 45° and the Intensity was measured for Analyser angles of $0^\circ, 45^\circ, 90^\circ$ and -45° over a range of Incident Angle from 20° to 60° . The larger the range of Angle of Incidence the better as it allows for a more representative fit to the model, however there is a hard lower limit determined by interference of the ellipsometer components and at higher angles the laser beam begins to spread out over the sample, which isn't ideal as effects such as in-homogeneity of the sample can start to effect the results. Once the values for the ellipsometry angles are calculated the next step is fitting a model to them, and then extracting the values of interest from the model. It is possible to fit a model to the experimental data with neither Refractive index or thickness of the thin film known prior, however the model requires a guess at these values to begin its optimization therefore having a ballpark figure is important. However if one of the refractive index or film thickness is already known you can instead fit a model by purely varying the unknown parameter, this way will provide a more reliable fit.

The first sample measured was the silicon Wafer, the measurements alongside the fitted theoretical values for the Ellipsometry angles as a function of Angle of Incidence are shown in Figure 4.8. The model produced values for the refractive index of the oxide layer to be $\tilde{N}_{SiO_2} = 1.708 \pm 0.3 - 0.01i \pm 0.2i$ with a film thickness $d = 88 \pm 7\text{nm}$.

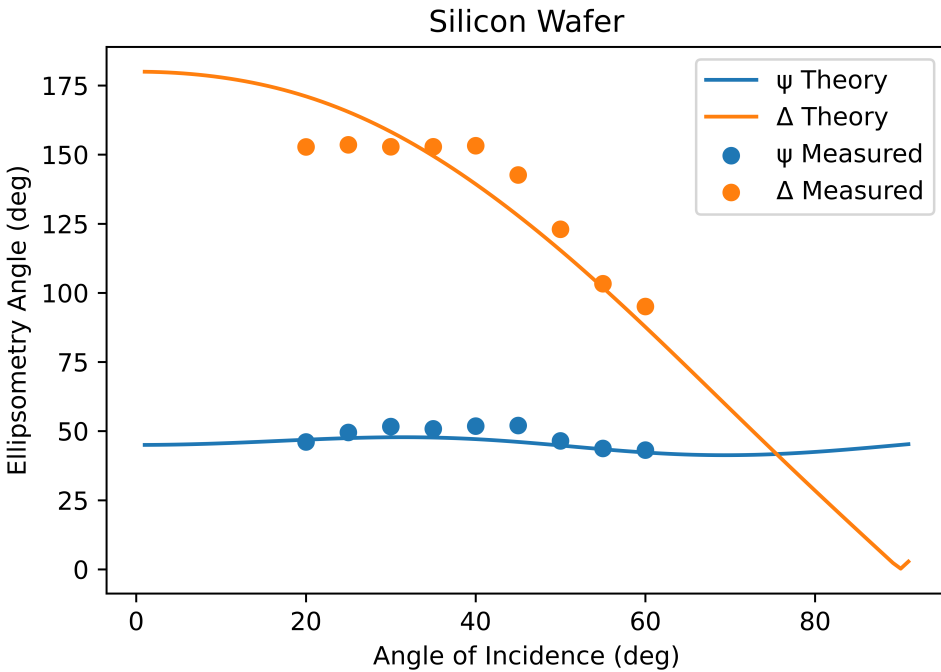


Figure 4.8: Variable angle of incidence measurements for a silicon wafer.

Measurements were also taken for the thin gold film on glass (Fig 4.9). Initially seeing as the refractive index of gold is known, the model was fit by varying only the film thickness which resulted in a thickness of $d = 27.3 \pm 4\text{nm}$. Subbing this value for d into the model fitter for known thickness we then obtained a refractive index of $\tilde{N}_{Au} = 0.0 \pm 0.1 + 2.5 \pm 0.1i$

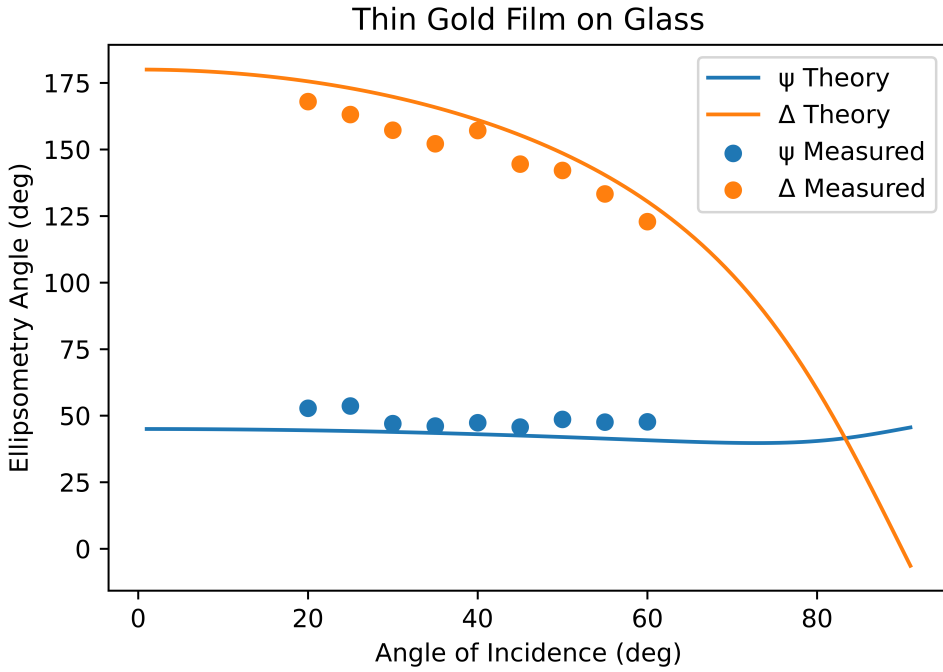


Figure 4.9: Variable angle of incidence measurements for a thin gold film on glass.

4.3 A note on Instrument Errors

For all the above plots of the collected data error bars have been omitted. The errors involved in the measurement of the intensities is reduced significantly by sampling on the order of a hundred samples and taking the average as the reading. The Incident Angles on the Ellipsometer are graded in single degree graduations, therefore any such measurements have an instrument error of half a degree. Finally the Analyser and Polariser are both rotated around with a worm drive with a ratio of 42 turns to one revolution, or approximately 8 degrees per revolution therefore the error is on the order of 0.1 degrees. All these errors are too small to be included in the plots of data.

4.4 Commercial Ellipsometer Measurements

The opportunity was presented to take some measurements with a commercial Variable Wavelength Ellipsometer. Which instead of varying incident angle and measuring intensities, vary the incident wavelength. This is far more convenient as there are fewer moving parts and hence fewer sources of error. It then produces plots of the ellipsometer angles as a function of wavelength. Models can then be fitted to these plots, in a similar manner to how we fit models to our plots of the ellipsometry angles over incident angle. The values of interest can then be extracted from these models. This particular Variable wavelength ellipsometer had an incident angle of 74.89°

Measurements were taken for the Thin gold Film on glass(Fig 4.10). A model was created with known values for the refractive index and calculated the film thickness of the gold to be $d = 29.2 \pm .3\text{nm}$

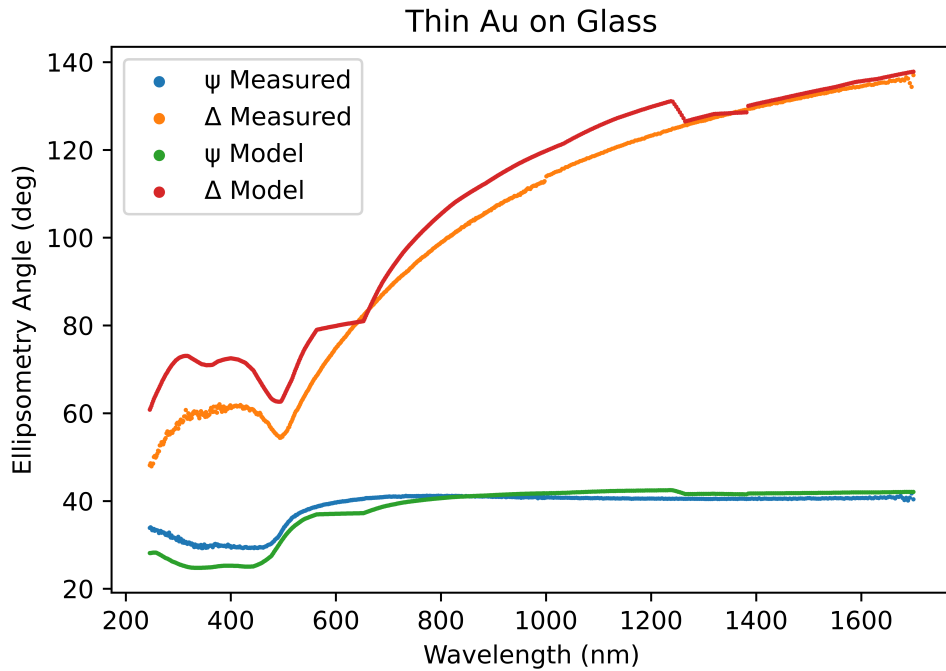


Figure 4.10: Variable wavelength ellipsometry measurements for a thin gold film on glass taken with a commercial ellipsometer.

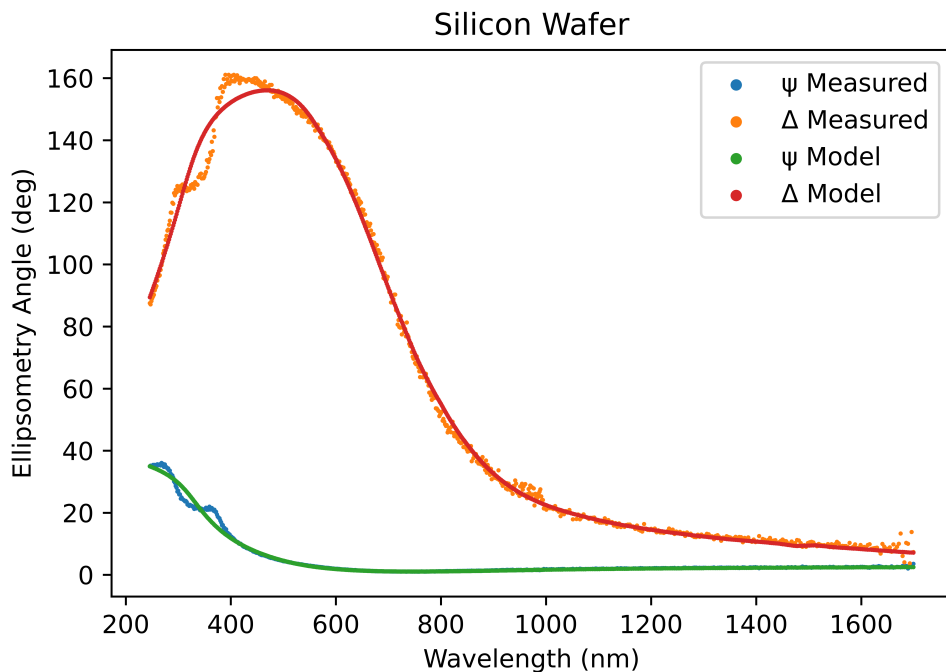


Figure 4.11: Variable wavelength ellipsometry measurements for a silicon wafer taken with a commercial ellipsometer.

Measurements were also taken for the silicon wafer using the commercial ellipsometer and are shown in Figure 4.11. The model fitted to the silicon wafer returned a value for the oxide thickness of $d = 62.4 \pm 0.2\text{nm}$

5 Discussion

A summary of the calculated complex refractive indices alongside there known values[1][17] for the range of samples tested with fixed AoI measurements is presented in the table below. The most accurate reading here for gold seems to be the thick gold on mica, which the calculated refractive index agreed to within 40% of the known value and the extinction coefficient to within 9%. Overall the readings for the extinction coefficients were closer to the known values for gold than the Refractive indices. The readings for the Gold layer on silicon are the furthest from the known values with a percentage error on n of 83% and over 100% on k, this is most probably due to the titanium layer not being factored into the model.

Table 5.1: Summary of results obtained from Fixed Angle of Incidence measurements using the 3D printed ellipsometer.

Sample	Calculated n:	Calculated k:	Known n:	Known k:
Glass	1.46 ± 0.07	0	1.51	0
Thick Gold on Mica	0.26 ± 0.04	3.3 ± 0.2	0.15557	3.6024
Thin Gold on Glass	0.42 ± 0.08	3.6 ± 0.2	0.15557	3.6024
Thick Gold on Glass	0.52 ± 0.07	3.15 ± 0.1	0.15557	3.6024
Thick Gold on Silicon	0.96 ± 0.1	1.74 ± 0.06	0.15557	3.6024
Silicon Oxide on Silicon	1.68 ± 0.1	0.44 ± 0.2	1.4565	0

A table of the calculated complex refractive indices and film thickness for the samples tested with the Variable Angle of Incidence are shown in Table 5.2. Along with the film thicknesses as calculated with the Commercial ellipsometer. The measurements for the gold film thickness agree within the experimental error to those measured by the commercial ellipsometer. Interestingly the refractive index measurements aren't as close as those measured using a Fixed Incident Angle. The Thickness of the silicon oxide layer measured using the 3D printed ellipsometer disagree with the commercial readings by about 43%.

Table 5.2: Summary of results obtained from Fixed Angle of Incidence measurements using the 3D printed ellipsometer.

Sample	Calculated		Known		Film Thickness d(nm) :	
	n:	k:	n:	k:	3D	Commercial
Thin Gold on Glass	0 ± 0.1	2.5 ± 0.1	0.15557	3.6024	27 ± 4	29.2 ± 0.3
Silicon Oxide on Silicon	1.68 ± 0.1	0.44 ± 0.2	1.4565	0	88 ± 7	61.7 ± 0.4

5.1 Factors Effecting Measurements

There are several factors that can affect the readings and skew the predicted values for refractive index and film thickness. Firstly it is important that the sample is oriented correctly in the ellipsometer so that the plane of incidence of the laser is perpendicular to the sample. The printed ellipsometer sample mount is oriented correctly, however there is a small amount of play in the system. To reduce the risk of this effecting readings interacting with the sample mount during readings was avoided. Secondly the point of incidence of the laser on the sample plays an important role in the measurements. If the sample is inhomogenous in any way the ellipsometer measurements will differ depending on the lasers incident location, this may be a reason why some of the readings from the commercial ellipsometer differed so much from that of the 3D printed instrument. Also this will affect the results for multiple measurements of the same material.

6 Conclusion

Based on the designs in the paper[4] a Rotating Angular Ellipsometer was 3D printed using an Ultimaker 2+ printer. The Ellipsometer design was adapted using 3D modelling software to fit a silicon photodiode and a small laser. The Ellipsometer components were assembled. Utilising the Brewster's angle the p and s orientations of the polarisers were determined. Measurements were then taken of laser intensity through the two polarisers as a function of polariser angle to ensure the linearity of the detector. A thin gold film was deposited on a glass slide using evaporation deposition. This sample, along with several others, were then measured using the 3D printed ellipsometer with fixed angle of incidence ellipsometry and variable angle of incidence ellipsometry.

Python code was then written to create theoretical plots of the ellipsometry angles as a function of angle of incidence. Code was also written to compute, from the intensity measurements, the ellipsometry angles for both fixed and variable angle of incidence measurements. Further code was written to fit a theoretical model of the ellipsometry angles to the experimental values and return the optical constants of the material. This model fitting code was adapted to be able to fit a model to measurements with known refractive indices or known film thickness and return the unknown parameter.

Finally Measurements were taken with a commercial ellipsometer and there values compared to those taken with the 3D printed instrument.

Values calculated using the Fixed Angle of Incidence measurements in the best case agreed with the known results to within 43% for the refractive index and 9% with the extinction coefficient. For the Variable angle ellipsometry measurements the film thickness of a gold film was measured and agreed with the measurements taken by a commercial ellipsometer within the limits of experimental error.

Overall the results indicate the viability of using a 3D printed instrument in taking both readings for complex refractive indices and film thicknesses. There is certainly room for improvements however. Firstly adapting the ellipsometer to accommodate a larger range of incident angle would increase the accuracy of the fitted model and hence provide more accuracy in the optical constants measured. Further improvements could be made in choosing a laser wavelength for the ellipsometer that is associated with the largest variation in the ellipsometer angles for the sample in question. The more the theoretical

model differs as a function of angle of incidence the more precision can be obtained in fitting the correct model.

7 References

- [1] P. B. Johnson and R. W. Christy. Optical Constants of the Noble Metals. *Physical Review B*, 6(12):4370–4379, December 1972. Publisher: American Physical Society.
- [2] Harland G. Tompkins. *A user's guide to ellipsometry*. Academic Press, Boston, 1993.
- [3] R. M. A. Azzam and N. M. Bashara. *Ellipsometry and polarized light*. North-Holland Pub. Co. ; sole distributors for the U.S.A. and Canada, Elsevier North-Holland, Amsterdam ; New York : New York, 1977.
- [4] Matthew Mantia and Teresa Bixby. Optical measurements on a budget: A 3D-printed ellipsometer. *American Journal of Physics*, 90(6):445–451, June 2022.
- [5] William Spottiswoode. *Polarisation of light*. Cambridge University Press, Cambridge, 2015. OCLC: 912414011.
- [6] P. Sivasankaran and B. Radjaram. 3D Printing and Its Importance in Engineering - A Review. In *2020 International Conference on System, Computation, Automation and Networking (ICSCAN)*, pages 1–3, Pondicherry, India, July 2020. IEEE.
- [7] Simon Ford and Tim Minshall. Invited review article: Where and how 3D printing is used in teaching and education. *Additive Manufacturing*, 25:131–150, January 2019.
- [8] Benjamin Schmidt, David King, and James Kariuki. Designing and Using 3D-Printed Components That Allow Students To Fabricate Low-Cost, Adaptable, Disposable, and Reliable Ag/AgCl Reference Electrodes. *Journal of Chemical Education*, 95(11):2076–2080, November 2018.
- [9] Mariano Calcabrini and Diego Onna. Exploring the Gel State: Optical Determination of Gelation Times and Transport Properties of Gels with an Inexpensive 3D-Printed Spectrophotometer. *Journal of Chemical Education*, 96(1):116–123, January 2019.
- [10] Jan Prikryl and Frantisek Foret. Fluorescence Detector for Capillary Separations Fabricated by 3D Printing. *Analytical Chemistry*, 86(24):11951–11956, December 2014.
- [11] Lon A. Porter, Benjamin M. Washer, Mazin H. Hakim, and Richard F. Dallinger. User-Friendly 3D Printed Colorimeter Models for Student Exploration of Instrument Design and Performance. *Journal of Chemical Education*, 93(7):1305–1309, July 2016.
- [12] Mihails Delmans and Jim Haseloff. μ Cube: a framework for 3D printable optomechanics. *Journal of Open Hardware*, 2018. ISBN: 2514-1708 Publisher: Ubiquity Press.
- [13] E. Brekke, T. Bennett, H. Rook, and E. L. Hazlett. 3D printing an external-cavity diode laser housing. *American Journal of Physics*, 88(12):1170–1174, December 2020.

- [14] Christian Scholz, Achim Sack, Michael Heckel, and Thorsten Pöschel. Inexpensive Mie scattering experiment for the classroom manufactured by 3D printing. *European Journal of Physics*, 37(5):055305, September 2016.
- [15] Beth Schaefer, Edward Collett, and Robert Smyth. Measuring the Stokes polarization parameters. *Am. J. Phys.*, 75(2), 2007.
- [16] Christian Negara. Fast Polarization State Detection by Division-of-Amplitude in a Simple Configuration Setup. 2016.
- [17] I. H. Malitson. Interspecimen Comparison of the Refractive Index of Fused Silica*,†. *Journal of the Optical Society of America*, 55(10):1205–1209, October 1965. Publisher: Optica Publishing Group.

8 Appendices

8.1 Appendix 1: Risk Assessment

Student Name:	Ishka Ó Cathluain
Student Number:	19449436
Project Title:	Construction and Testing of a 3D Printed Ellipsometer on a Budget
Main Working Location:	N204
Supervisor Name:	Dr. Paul Swift
Brief Listing of All Risks Associated with Project:	
<ul style="list-style-type: none">• General hazards of operating a low power laser• Inhaling PLA fumes• General hazards of moving heavy equipment• General hazards of using low power voltage	

Student:

I have attempted, to the best of my ability, to assess the risks associated with my project and to suggest appropriate controls and other measures to reduce the risk level. I have also consulted with my supervisor in performing and completing this risk assessment. I will implement these controls and other measures to reduce the risk level consistently throughout my project and make my supervisor aware if at any stage I feel the current risk assessment is insufficient as the project evolves.

Student Name: Ishka Ó Cathluain

Student Number: 19449436

Signature: Submission of this document is equivalent to a signature.

Date: 11/11/22

Supervisor:

I confirm that the student has undertaken a risk assessment of their project work and that they have consulted with me on this matter. Furthermore, the assessment above appears thorough and I will inform the student if at any stage I feel the current risk assessment is insufficient as the project evolves.

Supervisor Name: Dr. Paul Swift

Signature: Submission of this document is contingent upon supervisor's approval and implies it has been sort and approved.

Date: 11/11/22

8.2 Appendix 2: Python Scripts

```
# Model Fitting Code for the complex refractive index and film thickness for a three interface medium

#Coded based on ELLIPSOMETRY AND POLARIZED LIGHT by R. M. A. AZZAM and N. M. BASHARA

# assuming isotropic materials
# input file is a csv with the first column consisting of Angle of Incidence the next column the
# values for Psi and the last column Delta

import numpy as np
import matplotlib.pyplot as plt
import csv
from scipy.optimize import minimize

Psi_exp = []
Delta_exp = []

header = []
Series_Label = ''
Graph_Title = 'title'
CSV_file_location = 'Exp data.csv'
Dot_Size = 3

with open(CSV_file_location , 'r') as csvfile:
    header = next(csvfile).split(',')
    plots = csv.reader(csvfile, delimiter=',')
    X_title = ''
    Y_title = ''
    for row in plots:
        Psi_exp.append(float(row[1]))
        Delta_exp.append(float(row[2]))

def Delta(phi_0_DEG, N_1_real, N_1_imag, d):
    wavelength = 650e-9
    N_0 = 1 # refractive index of initial medium (air)
    N_2 = 1.5 # Refractive index of substrate
    N_1 = N_1_real + N_1_imag*1j #refractive index of thin film
    phi_0 = np.deg2rad(phi_0_DEG)
    phi_1 = np.arcsin(N_0*np.sin(phi_0)/N_1)
    phi_2 = np.arcsin(N_1*np.sin(phi_1)/N_2)
```

```

    r_01p = (N_1*np.cos(phi_0) - N_0*np.cos(phi_1)) / (N_1*np.
    ↵cos(phi_0) + N_0*np.cos(phi_1))
    r_12p = (N_2*np.cos(phi_1) - N_1*np.cos(phi_2)) / (N_2*np.
    ↵cos(phi_1) + N_1*np.cos(phi_2))
    r_01s = (N_0*np.cos(phi_0) - N_1*np.cos(phi_1)) / (N_0*np.
    ↵cos(phi_0) + N_1*np.cos(phi_1))
    r_12s = (N_1*np.cos(phi_1) - N_2*np.cos(phi_2)) / (N_1*np.
    ↵cos(phi_1) + N_2*np.cos(phi_2))

    Beta = 2 * np.pi * (d / wavelength) * N_1 * np.cos(phi_1)

    # Reflection Coefficients for p and s waves
    R_p =( r_01p + r_12p * np.exp(-2j*Beta) )/( 1 + r_01p * r_12p * np.
    ↵exp(-2j*Beta))
    R_s =( r_01s + r_12s * np.exp(-2j*Beta) )/( 1 + r_01s * r_12s * np.
    ↵exp(-2j*Beta))

    rho = R_p / R_s
    Delta = np.angle(rho,deg=True)
    return(Delta)

def Psi(phi_0_DEG, N_1_real, N_1_imag, d):
    wavelength = 650e-9
    N_0 = 1
    N_2 = 1.5
    N_1 = N_1_real + N_1_imag*1j

    phi_0 = np.deg2rad(phi_0_DEG)
    phi_1 = np.arcsin((N_0*np.sin(phi_0))/N_1)
    phi_2 = np.arcsin((N_1*np.sin(phi_1))/N_2)

    r_01p = (N_1*np.cos(phi_0) - N_0*np.cos(phi_1)) / (N_1*np.
    ↵cos(phi_0) + N_0*np.cos(phi_1))
    r_12p = (N_2*np.cos(phi_1) - N_1*np.cos(phi_2)) / (N_2*np.
    ↵cos(phi_1) + N_1*np.cos(phi_2))
    r_01s = (N_0*np.cos(phi_0) - N_1*np.cos(phi_1)) / (N_0*np.
    ↵cos(phi_0) + N_1*np.cos(phi_1))
    r_12s = (N_1*np.cos(phi_1) - N_2*np.cos(phi_2)) / (N_1*np.
    ↵cos(phi_1) + N_2*np.cos(phi_2))

    Beta = 2 * np.pi * (d / wavelength) * N_1 * np.cos(phi_1)

    # Reflection Coefficients for p and s waves

```

```

R_p =( r_01p + r_12p * np.exp(-2j*Beta) )/( 1 + r_01p * r_12p * np.
˓→exp(-2j*Beta))
R_s =( r_01s + r_12s * np.exp(-2j*Beta) )/( 1 + r_01s * r_12s * np.
˓→exp(-2j*Beta))

rho = R_p / R_s
Psi = np.degrees(np.arctan(np.absolute(rho)))
return(Psi)

phi_0_DEG = (20,25,30,35,40,45,50,55,60) #List of incedent angles

def residual(x):
    N_1_real = x[0]
    N_1_imag = x[1]
    d = x[2]
    Psi_pred = Psi(phi_0_DEG, N_1_real,N_1_imag , d)
    Delta_pred = Delta(phi_0_DEG, N_1_real, N_1_imag, d)
    err1 = np.mean((Psi_exp - Psi_pred)**2)
    err2 = np.mean((Delta_exp - Delta_pred)**2)
    error = (err1 + err2) / 2
    return error

x0 = [ 0.156, 3.6 ,10e-9] # initial guess for N_1 and d

res = minimize(residual, x0,bounds=[(0,None),(0,None),(0,None)],metho
˓→d="Nelder-Mead")
print('n:',res.x[0],'\n k:',res.x[1],'\n d:',res.x[2])

AoI_range = np.linspace(0, 91,100)
Delta_plot = Delta(AoI_range, res.x[0], res.x[1], res.x[2])
Psi_plot = Psi(AoI_range, res.x[0], res.x[1], res.x[2])

plt.figure()
plt.plot(AoI_range,Psi_plot,label='ψ Theory')
plt.xlabel('Angle of Incidence (deg)')
plt.ylabel('Ellipsometry Angle (deg)')
plt.plot(AoI_range,Delta_plot,label='Δ Theory')
plt.scatter(phi_0_DEG,Psi_exp,label='ψ Measured')
plt.scatter(phi_0_DEG,Delta_exp,label='Δ Measured')
plt.legend()
plt.title('Model Plot with Fitted data')
plt.show()

```

```

#Code Plotting Theoretical values for the ellipsometry equations as a
#function of Angle of Incidence for a two interface medium

#Coded based on ELLIPSOMETRY AND POLARIZED LIGHT by R. M. A. AZZAM and
→N. M. BASHARA

# assuming isotropic materials

import numpy as np
import matplotlib.pyplot as plt

wavelength = 546.1e-9 # wavelength of light

phi_0 = np.linspace(1,90,100)

phi_0_radians = np.radians(phi_0) # incident angle in medium 0
N_0 = 1 # refractive index of ambient medium (air)
N_1 = 3.8515 - 0.016460j # refractive index of substrate

# Use Snells law to find phi_1 and phi_2

phi_1 = np.arcsin(N_0*np.sin(phi_0_radians)/N_1)

# Fresnel Equations for s and p polarised light at the different
→interfaces

r_01p = (N_1*np.cos(phi_0_radians) - N_0*np.cos(phi_1)) / (N_1*np.
→cos(phi_0_radians) + N_0*np.cos(phi_1))
r_01s = (N_0*np.cos(phi_0_radians) - N_1*np.cos(phi_1)) / (N_0*np.
→cos(phi_0_radians) + N_1*np.cos(phi_1))

rho = r_01p / r_01s

#Psi = np.rad2deg(np.arctan(rho))
Psi = np.rad2deg(np.arctan(np.absolute(rho)))
Delta = np.angle(rho)
Delta = np.rad2deg(Delta)

plt.figure(0)

```

```

plt.plot(phi_0,Psi,label='ψ')
plt.xlabel('Angle of Incidence')
plt.ylabel('Psi')

plt.xlabel('Angle of Incidence (deg)')
plt.ylabel('Ellipsometry Angle (deg)')
plt.plot(phi_0,Delta,label='Δ')
plt.legend()
plt.title('Two Interface Medium')

plt.show

```

```

#Code Plotting Theoretical values for the ellipsometry equations as a function of Angle of Incidence for a three interface medium
#Coded based on ELLIPSOMETRY AND POLARIZED LIGHT by R. M. A. AZZAM and N. M. BASHARA

# assuming isotropic materials

# assuming isotropic materials

import numpy as np
import matplotlib.pyplot as plt

wavelength = 546.1e-9 # wavelength of light

phi_0 = np.linspace(1,90,100)

phi_0_radians = np.radians(phi_0) # incident angle in medium 0
N_0 = 1 # refractive index of ambient medium (air)
N_1 = 3.8515 - 0.016460j # refractive index of substrate

# Use Snells law to find phi_1 and phi_2

phi_1 = np.arcsin(N_0*np.sin(phi_0_radians)/N_1)

```

```

# Fresnel Equations for s and p polarised light at the different interfaces
r_01p = (N_1*np.cos(phi_0_radians) - N_0*np.cos(phi_1)) / (N_1*np.cos(phi_0_radians) + N_0*np.cos(phi_1))
r_01s = (N_0*np.cos(phi_0_radians) - N_1*np.cos(phi_1)) / (N_0*np.cos(phi_0_radians) + N_1*np.cos(phi_1))

rho = r_01p / r_01s

#Psi = np.rad2deg(np.arctan(rho))
Psi = np.rad2deg(np.arctan(np.absolute(rho)))
Delta = np.angle(rho)
Delta = np.rad2deg(Delta)

plt.figure(0)
plt.plot(phi_0,Psi,label='Ψ')
plt.xlabel('Angle of Incidence')
plt.ylabel('Psi')

plt.xlabel('Angle of Incidence (deg)')
plt.ylabel('Ellipsometry Angle (deg)')
plt.plot(phi_0,Delta,label='Δ')
plt.legend()
plt.title('Three Interface Medium')

plt.show

```

```

#Fixed AoI plots of Intensity vs Analyser Angle for a three interface medium

#Coded based on ELLIPSOMETRY AND POLARIZED LIGHT by R. M. A. AZZAM and N. M. BASHARA

# assuming isotropic materials

import numpy as np
import matplotlib.pyplot as plt

wavelength = 650e-9 # wavelength of light

```

```

phi_0_DEG = 45
phi_0 = np.deg2rad(phi_0_DEG)
N_0 = 1.000 # refractive index of ambient medium (air)
N_1 = 0.15557 + 3.6024j # refractive index of thin film
N_2 = 1.5 #refractive index of Substrate
d = 10e-9 # Film thickness
analyser_angle = np.linspace(0,np.pi*2,300)
pol_angle = np.radians(45)

# Use Snells law to find phi_1 and phi_2

phi_1 = np.arcsin(N_0*np.sin(phi_0)/N_1)
phi_2 = np.arcsin(N_1*np.sin(phi_1)/N_2)

# Fresnel Equations for s and p polarised light at the different interfaces
r_01p = (N_1*np.cos(phi_0) - N_0*np.cos(phi_1)) / (N_1*np.cos(phi_0) + N_0*np.cos(phi_1))
r_12p = (N_2*np.cos(phi_1) - N_1*np.cos(phi_2)) / (N_2*np.cos(phi_1) + N_1*np.cos(phi_2))
r_01s = (N_0*np.cos(phi_0) - N_1*np.cos(phi_1)) / (N_0*np.cos(phi_0) + N_1*np.cos(phi_1))
r_12s = (N_1*np.cos(phi_1) - N_2*np.cos(phi_2)) / (N_1*np.cos(phi_1) + N_2*np.cos(phi_2))

Beta = 2 * np.pi * (d / wavelength) * N_1 * np.cos(phi_1)

# Reflection Coefficients for p and s waves
R_p = r_01p + r_12p * np.exp(-2j*Beta) / 1 + r_01p * r_12p * np.exp(-2j*Beta)
R_s = r_01s + r_12s * np.exp(-2j*Beta) / 1 + r_01s * r_12s * np.exp(-2j*Beta)

rho = R_p / R_s

Psi = np.arctan(np.absolute(rho))
Delta = np.angle(rho)

Psi_prime = np.arctan(np.tan(Psi)/np.tan(pol_angle))

S_0 = 1

S_1 = - np.cos(2*Psi_prime)

```

```

S_2 = np.sin(2*Psi_prime)*np.cos(Delta)

I = .5*(S_0 + S_1*np.cos(2*analyser_angle)+S_2*np.sin(2*analyser_angle))

plt.figure(0)
plt.plot(np.degrees(analyser_angle),I)
plt.xlabel('Analyser Angle (deg)')
plt.ylabel('Intensity(%)')
plt.show()

```

*#Fixed analyser angle plots of Intensity vs Angle of incidence for a
three interface medium*

*#Coded based on ELLIPSOMETRY AND POLARIZED LIGHT by R. M. A. AZZAM and
N. M. BASHARA*

assuming isotropic materials

```

import numpy as np
import matplotlib
import matplotlib.pyplot as plt

wavelength = 650e-9 # wavelength of light

phi_0_DEG = np.linspace(1,91,100) # incident angle in medium 1 (air),  
# currently sweeping over angles from 0 to 90 deg
phi_0 = np.deg2rad(phi_0_DEG)

N_0 = 1.000 # refractive index of ambient medium (air)
N_1 = 0.15557 + 3.6024j # refractive index of thin film
N_2 = 1.5 #refractive index of Substrate
d = 10e-9 # Film thickness
analyser_angle = np.radians(68.57)
pol_angle = np.radians(45)

# Use Snells law to find phi_1 and phi_2

phi_1 = np.arcsin(N_0*np.sin(phi_0)/N_1)
phi_2 = np.arcsin(N_1*np.sin(phi_1)/N_2)

```

```

# Fresnel Equations for s and p polarised light at the different interfaces
r_01p = (N_1*np.cos(phi_0) - N_0*np.cos(phi_1)) / (N_1*np.cos(phi_0) + N_0*np.cos(phi_1))
r_12p = (N_2*np.cos(phi_1) - N_1*np.cos(phi_2)) / (N_2*np.cos(phi_1) + N_1*np.cos(phi_2))
r_01s = (N_0*np.cos(phi_0) - N_1*np.cos(phi_1)) / (N_0*np.cos(phi_0) + N_1*np.cos(phi_1))
r_12s = (N_1*np.cos(phi_1) - N_2*np.cos(phi_2)) / (N_1*np.cos(phi_1) + N_2*np.cos(phi_2))

Beta = 2 * np.pi * (d / wavelength) * N_1 * np.cos(phi_1)

# Reflection Coefficients for p and s waves
R_p = r_01p + r_12p * np.exp(-2j*Beta) / 1 + r_01p * r_12p * np.exp(-2j*Beta)
R_s = r_01s + r_12s * np.exp(-2j*Beta) / 1 + r_01s * r_12s * np.exp(-2j*Beta)

rho = R_p / R_s

Psi = np.arctan(np.absolute(rho))
Delta = np.angle(rho)

Psi_prime = np.arctan(np.tan(Psi)/np.tan(pol_angle))

S_0 = 1

S_1 = - np.cos(2*Psi_prime)
S_2 = np.sin(2*Psi_prime)*np.cos(Delta)

I = .5*(S_0 + S_1*np.cos(2*analyser_angle)+S_2*np.sin(2*analyser_angle)) # Transmitted Intensity / Incident Intensity

plt.figure(0)
plt.plot(np.degrees(phi_0),I)
plt.xlabel('Incident Angle (deg)')
plt.ylabel('Intensity(%)')

plt.show()

```

```

#Calculates refractive index from Psi and Delta

#Coded based on ELLIPSOMETRY AND POLARIZED LIGHT by R. M. A. AZZAM and
→ N. M. BASHARA

import numpy as np

incident_angle = 45

Psi_deg = 0.808*np.pi/180

Delta_deg = 2.6616*np.pi/180
n_0 = 1

def E1_E2(Psi_deg,Delta_deg,n_0,incident_angle):
    E_1 = (n_0 * np.sin(incident_angle))**0.5*(1+((np.
    ↪ tan(incident_angle)**2)*(np.cos(2*Psi_deg))**2-(np.
    ↪ sin(2*Psi_deg))**2*np.sin(Delta_deg)**2)/(1+np.sin(2*Psi_deg)*np.
    ↪ cos(Delta_deg))**2)
    E_2 = -((n_0*np.sin(incident_angle)*np.tan(incident_angle))**2*np.
    ↪ sin(4*Psi_deg)*np.sin(Delta_deg))/(1+np.sin(2*Psi_deg)*np.
    ↪ cos(Delta_deg))**2
    return (E_1,E_2)

def refractive_index(E_1,E_2):
    n_1 = (.5*(E_1**2+E_2**2)**.5+E_1)**.5
    k_1 = (.5*(E_1**2+E_2**2)**.5-E_1)
    return(n_1,k_1)

E_1 = E1_E2(Psi_deg, Delta_deg, n_0, incident_angle)[0]
E_2 = E1_E2(Psi_deg, Delta_deg, n_0, incident_angle)[1]
result = refractive_index(E_1, E_2)
print('n =',result[0], ' k =',result[1], ' i')

```